Available online at www.sciencedirect.com
SCIENCE DIRECT®
Thermochimica Acta 434 (2005) 55–61
thermochimica acta
www.elsevier.com/locate/tca

Characterization of monofunctional ZrO_2–MoO_3 catalysts for methylcyclopentane conversion

Carolyn Kenney, Yadollah Maham, Alan E. Nelson*

University of Alberta, Department of Chemical and Materials Engineering, Edmonton, Alta., Canada T6G 2G6

Received 30 August 2004; received in revised form 10 December 2004; accepted 30 December 2004
Available online 30 January 2005

Abstract

A series of ZrO_2–MoO_3 catalysts with different molybdenum loadings (0–18.7 at.% Mo) prepared by co-precipitation were characterized and evaluated for their performance for methylcyclopentane (mcp) conversion. The dependence of Mo content on the crystallinity, surface area, and acidic properties of ZrO_2–MoO_3 is studied and evaluated as a function of molybdenum loading. The monoclinic phase is observed at low Mo loadings, with the tetragonal polymorph of ZrO_2 effectively stabilized at higher Mo loadings. The surface area of ZrO_2–MoO_3 increases with molybdenum content to a maximum value of 124 $m^2\ g^{-1}$ at a loading of 15.8 at.% Mo, followed by a decrease at higher Mo loadings. Isothermal CO_2 adsorption and ammonia TPD results indicate the strength of basic sites and specific NH_3 desorption decreases with increasing molybdenum content, while TPR indicates ZrO_2–MoO_3 catalysts are more easily reduced with increasing molybdenum loading. The most active catalyst for mcp conversion (36% conversion) corresponds to a molybdenum loading of 3.2 at.% Mo, which has the highest acidity per surface area of the ZrO_2–MoO_3 catalysts studied.

Keywords: Zirconium; Molybdenum; Oxide; Structure; Acidity; Methylcyclopentane

1. Introduction

Traditionally, the octane number of gasoline fuels has been improved by the addition of aromatic compounds [1–3]; however, aromatics are becoming less suitable for this purpose because of new legislation set by the European Auto Oil Programme and other global organizations [3]. Considerable work is being done to convert aromatics to high quality synthetic steamcracker feed (ethane, propane, and *n*-butane), and to cleaner distillate streams for the production of diesel fuels. However, with the increased utilization of heavy oils and vacuum residue, new catalysts are required to selectively hydrogenate the aromatics and polyaromatics of heavy oils to produce diesel fuels with lower aromatic content. Diesel fuels that contain lower concentrations of aromatics have higher cetane numbers, giving shorter ignition delays, smoother engine operation, more complete combustion, and less particulate matter in the exhaust gases [4,5].

Improving the cetane number of diesel fuels involves hydrotreatment over monofunctional or bifunctional catalysts to produce paraffins, olefins, and alkyl-substituted rings. Over monofunctional catalysts, ring-opening reactions are suggested to proceed via the Haag–Dessau mechanism, where alkanes are directly protonated to non-classical carbonium ions in the transition state [1]. The Haag–Dessau mechanism involves preferential cracking of the most highly branched carbon atom and high activation energies. Over bifunctional catalysts consisting of solid-acid supported metals, ring-opening reactions are suggested to proceed via isomerization of six-membered rings to five-membered rings on acidic sites followed by hydrogenation over metal sites [6]. One of the challenges of formulating an effective bifunctional catalyst is balancing the acidic and metallic functionality to produce linear alkanes without significant dealkylation.

* Corresponding author. Tel.: +1 780 492 7380; fax: +1 780 492 2881.
E-mail address: alan.nelson@ualberta.ca (A.E. Nelson).

0040-6031/$ – see front matter © 2005 Elsevier B.V. All rights reserved.
doi:10.1016/j.tca.2004.12.022

Combined with a second metal oxide, zirconia has many attractive catalytic properties including a strong interaction with active phases, acidic and basic functionality, and thermal and chemical stability [7]. Metal oxides such as MoO_3, WO_3, or CuO can be combined with ZrO_2 by wet-impregnation, sol-gel impregnation, or co-precipitation. The second metal oxide, as well as the method of preparation, can produce a zirconia-based catalyst with different chemical, physical, and catalytic properties. Previous work has shown that the incorporation of molybdenum with zirconia through co-precipitation yields mixed oxides that have a higher surface area and are more easily reduced [7–9], leading to higher catalytic activity.

The objective of the present study was to prepare and characterize a series of monofunctional ZrO_2–MoO_3 catalysts with a molybdenum loading from 0 to 20 at.% Mo. The catalysts were prepared by co-precipitation and characterized using X-ray photoelectron spectroscopy (XPS), synchrotron X-ray powder diffraction (SXPD), BET surface area, CO_2 isothermal adsorption, temperature-programmed reduction (TPR), and temperature-programmed desorption (TPD) of ammonia (NH_3). The activities of the ZrO_2–MoO_3 catalysts were evaluated using methylcyclopentane, and the correlations between catalyst properties and methylcyclopentane conversion are discussed.

2. Experimental methods

2.1. Preparation of ZrO_2–MoO_3

The synthesis of ZrO_2–MoO_3 catalysts was carried out by co-precipitation routines, similar to those detailed by Calafat et al. [9]. The solid precursors, zirconyl chloride octahydrate ($ZrOCl_2{\cdot}8H_2O$, Sigma–Aldrich, 98%) and ammonium heptamolybdate ($(NH_4)_6Mo_7O_{24}{\cdot}4H_2O$, Fisher Scientific, certified ACS), were combined using various amounts of molybdenum to achieve a final Mo loading from 0 to 20 at.%. The precursors were weighed, approximately 10 mL of de-ionized water was added, and the aqueous mixture was heated to completely dissolve the solids. Ammonium hydroxide (NH_4OH, Sigma Aldrich, 14.8 M ACS reagent) was added drop-wise until the pH was 9.25. The resulting solids were vacuum filtered and washed with five parts distilled water. The samples were dried at room temperature for 24 h, dried at 140 °C in air for 8 h, and calcined at 500 °C in flowing air for 2 h. The resulting mixed oxides are indicated as 0MoZr, 3.2MoZr, 4.7MoZr, 8.7MoZr, 10.8MoZr, 15.8MoZr, and 18.7MoZr in reference to the actual percentage (atomic) of Mo in each ZrO_2–MoO_3 catalyst.

2.2. Characterization of ZrO_2–MoO_3

2.2.1. Molybdenum loading

The atomic concentration of molybdenum in the ZrO_2–MoO_3 catalysts was determined by using X-ray photoelectron spectroscopy (XPS). XPS was performed using a Kratos Axis 165 spectrometer with monochromatic Al Kα radiation (1486.6 eV). Prior to analysis, the oxide powders were milled, formed into wafers (ca. 150 mg), and degassed for approximately 2 h at $<5 \times 10^{-9}$ Torr. Survey (wide) spectra were collected from 0 to 1100 eV with a pass energy of 160 eV, step size of 0.5 eV, and a dwell time of 0.15 s (single scan). Peak assignments and atomic concentrations were calculated using the algorithm and sensitivity factors contained in the Kratos Vision2 software.

2.2.2. Synchrotron X-ray powder diffraction (SXPD)

Synchrotron X-ray powder diffraction (SXPD) measurements were performed using the SUNY beamline X3B1 at the National Synchrotron Light Source (NSLS), Brookhaven National Laboratory (BNL). The synchrotron beam was monochromated by a double Si(1 1 1) crystal monochromator at a wavelength of 0.69952 Å, as calibrated from a series of seven well-defined reflections using a NIST corundum X-ray diffraction standard (NIST 1976a). The intensity of the incident beam was monitored by an ion chamber and normalized for the decay of the primary beam, and the diffracted beam was analyzed with a Ge(1 1 1) crystal. X-ray scattering intensities were collected at room temperature in steps of 0.01° by counting for 1 s at every 2θ from 5° to 55°.

2.2.3. Calorimetric CO_2 adsorption

Calorimetric CO_2 adsorption experiments were performed using a Setaram Differential Scanning Calorimeter DSC-111. Approximately 100 mg of sample was packed into a silica glass reactor tube on top of a sintered quartz substrate. The samples were heated to the adsorption temperature (100, 200, and 300 °C) at a rate of 15 °C min^{-1} under a flow of argon (99.99%, 1 L h^{-1}). Isothermal CO_2 adsorption was performed by dosing the samples with CO_2 (99.99%, 1.2 L h^{-1}) followed by out-gassing with argon. The heat released during adsorption was measured by a series of Seebeck-effect thermal junctions in μV and converted to mW through calibration with a Joule-effect device.

2.2.4. Surface area, TPR, and NH_3 TPD

Surface area measurements (BET), temperature-programmed reduction (TPR), and ammonia temperature-programmed desorption (TPD) were performed with an AutoChem II 2910 (Micromeritics) equipped with a thermal conductivity detector (TCD) at a sampling rate of 1 Hz. For surface area analysis, approximately 150 mg of sample was placed in the U-shaped quartz sample tube on a quartz wool bed and degassed in flowing helium (99.999%, 10 mL min^{-1}) at 250 °C for 30 min. After pretreatment, the BET surface area was measured using a 29.9% nitrogen/helium mixture. TPR measurements were performed using a similar pretreatment followed by sample heating from 25 to 500 °C at a heating rate of 10 °C min^{-1} in flow of 10% H_2/Ar (50 mL min^{-1}). Ammonia TPD analysis was performed by initially pretreating the samples at 200 °C for

Table 1
Predicted and experimental (XPS) composition data

Mo loading (at.%)		Atomic ratio (O/(Mo + Zr))	
Predicted	Experimental	Predicted[a]	Experimental[b]
0	0	2.00	2.18
2	3.2	2.03	2.26
5	4.7	2.05	2.36
7	8.7	2.09	2.40
10	10.8	2.11	2.41
15	15.8	2.16	2.50
20	18.7	2.19	2.37

[a] The predicted atomic ratio is based on the structural formula of ZrO_2–$yMoO_3$ calculated using the actual Mo loading.
[b] The excess surface oxygen is attributed to surface hydroxyl, CO, and CO_2 species.

60 min and then cooling to 80 °C for 10 min under helium (99.999%). After TPD pretreatment, the samples were dosed with 14.9% NH_3/He (15 mL min^{-1}) for 30 min. Ammonia was used as a probe molecule because of its stability, strong basic strength ($pK_a = 9.25$) and small size (0.3 nm) [10]. Excess ammonia was removed by passing helium (99.999%, 25 mL min^{-1}) over the sample for 60 min, and ammonia TPD was carried out from 80 to 500 °C at a heating rate of 10 °C min^{-1}.

2.3. Methylcyclopentane conversion

ZrO_2–MoO_3 reactivity studies were performed using methylcyclopentane (mcp) as a probe molecule to provide a measure of reactivity as a function of molybdenum substitution. Reactivity experiments were carried out at 300 °C and 101 kPa using a differential flow reactor. The relative concentration of methylcyclopentane was monitored with a Dycor Quadropole Gas Analyzer, and subsequently quantified by measuring the intensity of the mass-to-charge (*m*/*z*) ratio of 56. The samples were initially reduced in hydrogen using temperature-programmed reduction as previously discussed. The liquid methylcyclopentane was vaporized at a reflux temperature of 45 °C, flask temperature of 50 °C and a loop volume of 0.13 mL, and pulse-injected at an interval of 10 min to a carrier gas of 10% H_2/Ar (10 mL min^{-1}). The *m*/*z* (56) intensities of 8 mcp pulse injections were quantified, and mcp conversion was calculated based on the *m*/*z* (56) intensity in the absence of a catalyst.

3. Results and discussion

3.1. Composition and structural analysis

Table 1 presents the predicted and actual compositions of the ZrO_2–MoO_3 catalysts, as characterized by XPS. The actual molybdenum content is in good agreement with the predicted molybdenum loading; however, the XPS molybdenum content is usually higher than the predicted values. These differences may be attributed to several factors, including sample inhomogeniety, the incomplete dissolution of the precursors during sample preparation, or surface molybdenum enrichment. The measured O/(Mo + Zr) atomic ratios were also higher than theoretical values based on an empirical ZrO_2–MoO_3 formula considering the experimental Mo content, suggesting the presence of surface CO, CO_2, OH species.

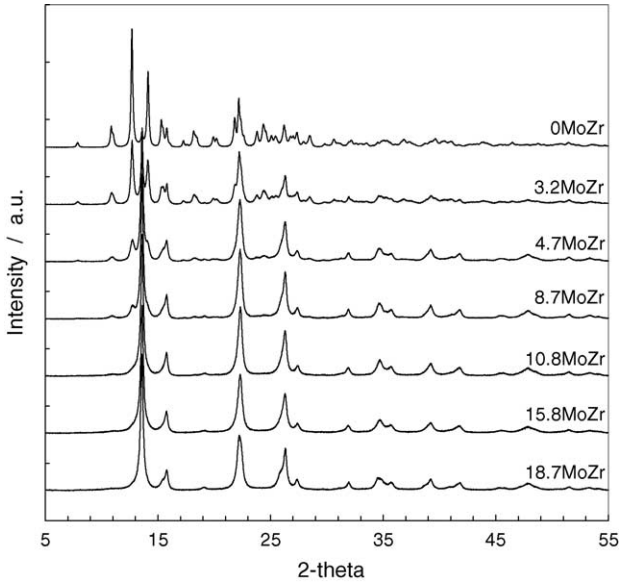

Fig. 1. Synchrotron X-ray powder diffraction (SXPD) patterns of ZrO_2–MoO_3. The data were collected at room temperature using a wavelength of 0.69952 Å, steps of 0.01°, and dwell time of 1 s.

ZrO_2 can exist in the monoclinic, tetragonal, and cubic phases depending on calcination temperature [11]; however, the stabilization of the tetragonal ZrO_2 phase is important for catalytic applications. In the present study, unpromoted ZrO_2 (0MoZr) exhibits a characteristic monoclinic diffraction pattern (Fig. 1). The addition of molybdenum leads to modification in the crystalline structure, indicating molybdenum effectively stabilizes the tetragonal polymorph of ZrO_2. The monoclinic structure is dominant at low Mo loadings, while higher molybdenum loadings above 4.7 at.% Mo (4.7MoZr) increased the proportion of the tetragonal phase, as evidenced by the reflection at approximately $2\theta = 14°$. The lack of discernible reflection peaks between $2\theta = 10°$–$13°$ ($\lambda = 0.69952$ Å) indicate the absence of a separate MoO_3 phase. These results are consistent with previous crystallographic studies of ZrO_2–MoO_3 that indicated the tetragonal phase is dominant at low Mo loadings [9]. It is believed that molybdenum opposes the tetragonal to monoclinic transition by decreasing the zirconia grains below a critical size and retarding the grain-growth rate. Zhao et al. [12] also noted that the broadening of the diffraction peaks for ZrO_2–MoO_3, as observed in the present study, indicates the ZrO_2 crystallite size is smaller while the tetragonal structure is retained.

Table 2 summarizes the crystalline structure and specific BET surface areas of ZrO_2–MoO_3 as a function of molybdenum content. For pure ZrO_2 (0MoZr), the specific sur-

Table 2
BET surface areas and crystallinity of ZrO_2–MoO_3

Mo loading (at.%)	S_g (BET) ($m^2\,g^{-1}$, ±5%)	Crystalline structure[a]
0	20	M
3.2	31	M(+), T(−)
4.7	63	M(−), T(+)
8.7	78	T
10.8	101	T
15.8	124	T
18.7	111	T

[a] M: monoclinic, T: tetragonal; (−) minor phase; (+) dominant phase.

face area was $20\,m^2\,g^{-1}$. The surface areas for ZrO_2–MoO_3 increased with increasing Mo loading to $124\,m^2\,g^{-1}$ for 15.8MoZr, followed by a decrease to $111\,m^2\,g^{-1}$ for 18.7MoZr. Comparable BET surface areas for ZrO_2–MoO_3 have been reported elsewhere [9,12]. The observed maximum in surface area as a function of molybdenum substitution is attributed to the ability of molybdenum to stabilize the zirconia grains. ZrO_2–MoO_3 catalysts prepared by methods other than co-precipitation, namely wet-impregnation, yield lower surface areas that decrease with molybdenum loading [8,13]. The results obtained from this study qualitatively agree with previous work, demonstrating that higher surface areas are obtained when catalysts are prepared by co-precipitation.

3.2. Temperature-programmed reduction and oxidation

Temperature-programmed reduction profiles for ZrO_2–MoO_3 are shown in Fig. 2. The total hydrogen uptake increased with increasing molybdenum loading, indicating the ZrO_2–MoO_3 catalysts are more reducible at higher molybdenum loadings. The 3.2MoZr catalyst showed a single reduction peak centered at approximately 395 °C. With increased molybdenum loading, a second reduction peak evolved and became more pronounced and shifted to lower temperatures, suggesting that reduction occurred in two stages and the catalysts were more easily reduced. The reduction peaks were fitted to determine H_2 uptake, and the resulting specific hydrogen uptake and peak temperatures as a function of Mo loading are located in Table 3. The TPR data is expressed in units of mL m^{-2} for direct comparison to CO_2 adsorption and mcp conversion results. As the Mo loading

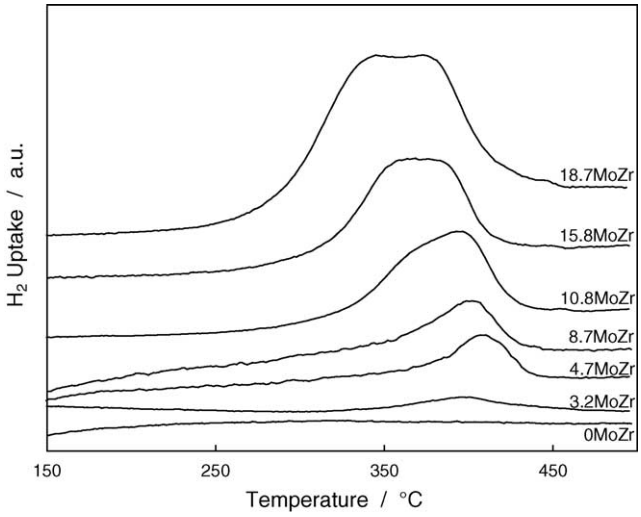

Fig. 2. Temperature-programmed reduction profiles of ZrO_2–MoO_3. TPR was performed from 25 to 500 °C at a heating rate of 10 °C min^{-1} in flow of 10% H_2/Ar (50 mL min^{-1}).

increased from 0MoZr to 4.7MoZr, the specific hydrogen uptake increased from 0 to 4.6×10^{-2} mL m^{-2}. The maximum total specific hydrogen uptake (15.0×10^{-2} mL m^{-2}) was observed for the 18.7MoZr sample, corresponding to the highest molybdenum loading in the present study.

The TPR analysis clearly indicated the presence of two reduction peaks at higher Mo loadings. Calafat et al. [9] also observed that the reduction of ZrO_2–MoO_3 catalysts occurred in two stages. The low temperature peak was assigned to the reduction of dispersed polymolybdates and the high temperature peak was assigned to the reduction of MoO_3 to MoO_2 [9]. Bhaskar et al. [7] found that reduction of MoO_3 to MoO_2 occurred at 767 °C while reduction of MoO_2 to Mo occurred at 987 °C. The peaks observed for the reduction of MoO_3 to MoO_2 by Calafat et al. [9] may have been lower because of Zr–O/Mo–O interactions, owing to the method of catalyst preparation (co-precipitation). However, the peak temperatures observed in the present study were all lower those previously reported for MoO_3 and MoO_2. Based on the reported temperatures for the reduction polymolybdates [9], the peaks observed in the present study may be assigned to the reduction of polymolybdates. The nature and concentration of surface Mo species is dependant on the Mo loading, and the observed

Table 3
Effect of Mo content on H_2 uptake

Mo loading (at.%)	H_2 uptake ($\times 10^{-2}$ mL m^{-2})		Total H_2 uptake ($\times 10^{-2}$ mL m^{-2})	Temperature (°C)	
	First peak	Second peak		First peak	Second peak
0	–	–	0	–	–
3.2	–	–	4.8	–	–
4.7	1.3	2.6	4.6	365	407
8.7	2.0	4.3	8.0	365	402
10.8	2.6	4.3	7.4	357	395
15.8	3.9	3.8	9.1	350	385
18.7	6.7	6.8	15.0	333	379

The first peak corresponds to the low-temperature peak and the second peak corresponds to the high-temperature peak, as fit using numerical routines.

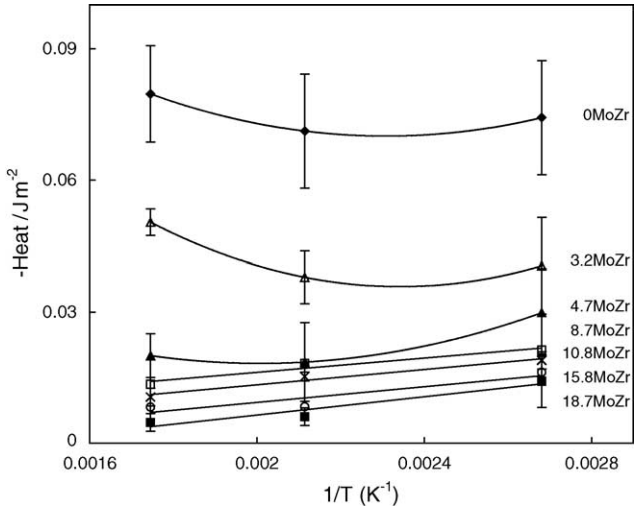

Fig. 3. Differential heats of isothermal CO_2 adsorption as a function of temperature for ZrO_2–MoO_3 catalysts.

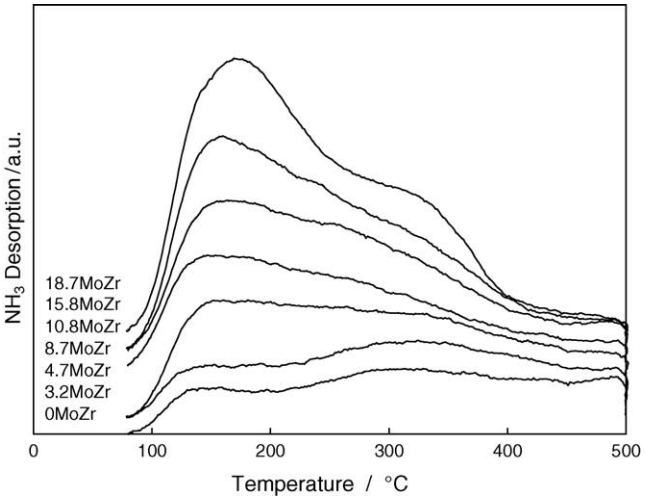

Fig. 4. Ammonia (NH_3) temperature-programmed desorption profiles of ZrO_2–MoO_3.

increase in the amount of H_2 consumed with increasing Mo loading is consistent with this argument.

Temperature-programmed oxidation (TPO) was performed to determine if the TPR process was reversible (results not shown). TPO of ZrO_2–MoO_3 showed that the oxygen uptake increased with Mo content, similar to the increase in hydrogen uptake. Catalysts that were subjected to TPR following TPO produced similar reduction profiles as untreated samples. The TPR results prior to and following treatment with TPO indicate reduction is completely reversible, as the reduced catalysts returned to their oxidized state during TPO.

3.3. CO_2 and NH_3 adsorption

Fig. 3 shows the isothermal heat of CO_2 adsorption at three different temperatures (100, 200, 300 °C) for each ZrO_2–MoO_3 catalyst. The surface basicity decreased with increasing molybdenum loading, as evidenced by the decreasing heats of CO_2 adsorption with increasing Mo loading. The strength of basic sites rapidly decreased from pure ZrO_2 (0.07 J m^{-2}) to a molybdenum loading of 4.7 at.% (0.03 J m^{-2}) at 100 °C. The effect of increased Mo loading from 10.8 to 18.7 at.% Mo was less pronounced, only decreasing the heat of CO_2 adsorption from 0.02 to 0.01 J m^{-2}, respectively, at 100 °C. When the ZrO_2–MoO_3 catalysts were subsequently dosed with CO_2, the heats of adsorption decreased indicating that the adsorption process was not completely reversible. The irreversible adsorption is an indication of surface inhomogeniety and the presence of different adsorption sites. CO_2 can react with basic oxygen species on the surface giving carbonate-like species that possess different structures on different crystalline phases. This is clearly evidenced by the differences in isothermal CO_2 adsorption as a function of Mo content, indicating surface basicity is dependent on the crystalline structure.

Ammonia temperature-programmed desorption (TPD) spectra profiles for ZrO_2–MoO_3 are shown in Fig. 4. The spectrum for each ZrO_2–MoO_3 catalyst suggests two NH_3 desorption peaks, corresponding to strong and moderate acidic sties. As can be seen by the increasing area under the curves, the number of acid sites increased with Mo loading (per mass). Irrespective of molybdenum loading, the first and second peak occurred at approximately 150 and 300 °C, respectively. The volume of ammonia desorbed per unit surface area is shown in Fig. 5. The desorbed volume per unit surface area decreased with molybdenum loading followed by an increase, with a minimum specific desorption volume at a Mo loading of 10.8 at.%. Overall, pure ZrO_2 demonstrated the highest NH_3 desorption volume (specific), while the addition of molybdenum clearly modifies the nature and concentration of the acidic sites.

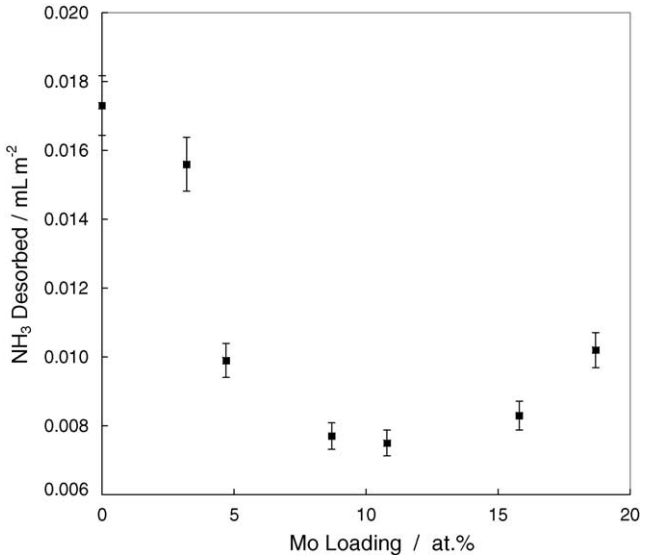

Fig. 5. Volume of ammonia desorbed (specific) as a function of Mo loading for ZrO_2–MoO_3.

Table 4
Conversion of methylcyclopentane (mcp) over ZrO_2–MoO_3

Mo loading (at.%)	mcp conversion
0	9
3.2	36
4.7	Negligible
8.7	3
10.8	9
15.8	Negligible
18.7	9

Li et al. [13] reported peaks of NH_3 desorption at 327 °C (SiO_2–Al_2O_3), 377 °C (H-ZSM-5), 427 °C (mordenite), and 557 °C ($Cs_{2.5}H_{0.5}PW_{12}O_{40}$). Preparation of ZrO_2–MoO_3 catalysts by different methods only appears to have an effect on the distribution and not the strength of acid sites. Bhaskar et al. [7] observed two ammonia TPD peaks at 300 and 550 °C that increased in intensity with increasing Mo-loading for catalysts prepared by incipient wetting of ZrO_2 and calcined at 500 °C. A single adsorption peak at approximately 200 °C was observed by Li et al. [13] for catalysts prepared by impregnation of $Zr(OH)_4$ and calcined at temperatures from 300 to 900 °C. In the present study, the first peak somewhat agrees with what has been reported by Li et al. (200 °C) [13] while the second peak agrees with what has been reported by Bhaskar et al. (300 °C) [7]. However, a detailed comparison between the results of the present study and those studied by Li et al. is not possible, because NH_3 desorption was limited to 500 °C in the present study to avoid structural changes. Thus, the influence of preparation method on the number and strength distribution of the strong acidic sites cannot be evaluated.

3.4. Methylcyclopentane conversion

Reaction studies were carried out using methylcyclopentane (mcp) as a model compound to evaluate the activity of the ZrO_2–MoO_3 catalysts (Table 4). The conversion of mcp is defined as the disappearance of mcp, and in the presence of H_2 would include both ring-opening and cracking reactions. The highest conversion of mcp (36%) over ZrO_2–MoO_3 catalyst was observed at a Mo loading of 3.2 at.%, corresponding to the ZrO_2–MoO_3 catalyst with the most acid sites per unit surface area. However, pure ZrO_2 with the highest concentration of acidic sites demonstrated only marginal mcp conversion, and ZrO_2–MoO_3 catalysts with different Mo content demonstrated only marginal mcp conversion (0–9%).

Various studies have found that as the surface acidity increases, catalyst activity and selectivity increases. For example, Bhaskar et al. [7] found that as the number of strong acid sites increased, the conversion of 3-picoline and the selectivity towards nicotinonitrile increased. Li et al. [13] concluded the catalytic activity of ZrO_2–MoO_3 for "water–tolerant catalysis" was governed partly by the acidic properties of the surface. As the calcination temperature was increased, the conversion in esterification and the density of NH_3 adsorbed on the surface increased [13]. Tanabe [14] reported that high catalytic activities and selectivities of ZrO_2–MoO_3 catalysts were explained by the interaction of weakly acidic sites with moderately basic sites. However, it is clear from the present studies that while surface acidity is an important factor governing catalytic activity, other factors contribute to ZrO_2–MoO_3 activity, namely reducibility and crystallinity.

Additional studies are being performed to identify the nature of the reaction products and ring-opening selectivity for the reaction of mcp over ZrO_2–MoO_3. A detailed reaction mechanism and reaction kinetics will be the subject of a forthcoming manuscript.

4. Conclusions

The characterization of ZrO_2–MoO_3 catalysts have shown that when molybdenum is incorporated with zirconia through co-precipitation, molybdenum stabilizes the tetragonal polymorph of ZrO_2, increases the specific surface area, decreases the strength of basic sites, increases the reducibility, and decreases the number of acidic sites per unit surface area. The increase in surface area was attributed to the ability of molybdenum to stabilize ZrO_2 grains below a critical size and prevent grain growth. In addition to the decrease in basicity strength that was observed with increasing Mo loading, it was observed that the CO_2 adsorption process was not completely reversible owing to the presence of different active sites. Temperature-programmed desorption profiles of ammonia exhibited two peaks, corresponding to the presence of moderate and strong acid sites. The reaction results indicate that the ZrO_2–MoO_3 catalyst with the highest acidity per surface area (3.2 at.% Mo) yields the highest mcp conversion (36%). Consequently, future studies of ZrO_2–MoO_3 ring opening catalysts will focus on low Mo loadings (below 10 at.%).

Acknowledgements

This work is supported by Syncrude Canada Ltd. and the Natural Sciences and Engineering Research Council (NSERC) under grant no. CRDPJ 266625. Research carried out (in whole or in part) at the National Synchrotron Light Source, Brookhaven National Laboratory, which is supported by the U.S. Department of Energy, Division of Materials Sciences and Division of Chemical Sciences, under Contract No. DE-AC02-98CH10886.

References

[1] J. Weitkamp, A. Raichle, Y. Traa, Appl. Catal. A 222 (2001) 277–297.
[2] A. Raichle, Y. Traa, J. Weitkamp, Appl. Catal. B 41 (2003) 193–205.
[3] C. Berger, A. Raichle, R.A. Rakoczy, Y. Traa, J. Weitkamp, Micropor. Mesopor. Mater. 59 (2003) 1–12.

[4] A. Corma, V. González-Alfaro, A.V. Orchillés, J. Catal. 200 (2001) 34–44.
[5] S. Albertazzi, R. Ganzerla, C. Gobbi, M. Lenarda, M. Mandreoli, E. Salatelli, P. Savini, L. Storaro, A. Vaccari, J. Mol. Catal. A 200 (2003) 261–270.
[6] G.B. McVicker, M. Daage, M.S. Touvelle, C.W. Hudson, D.P. Klein, W.C. Baird, B.R. Cook, J.G. Chen, S. Hanter, D.E.W. Vaughan, E.S. Ellis, O.C. Feeley, J. Catal. 210 (2002) 137–148.
[7] T. Bhaskar, K.R. Reddy, C.P. Kumar, M.R.V.S. Murthy, K.V.R. Chary, Appl. Catal. A 211 (2001) 189–201.
[8] S.K. Maity, M.S. Rana, B.N. Srinivas, S.K. Bej, G.M. Dhar, T.S.R. Prasada, J. Mol. Catal. A 153 (2000) 121–127.
[9] A. Calafat, L. Avilán, J. Aldana, Appl. Catal. A 201 (2000) 215–223.
[10] B. Dragoi, A. Gervasini, E. Dumitriu, A. Auroux, Thermochim. Acta 420 (2004) 127–134.
[11] E.J. Walter, S.P. Lewis, A.M. Rappe, Surf. Sci. 495 (2001) 44–50.
[12] B.Y. Zhao, X.P. Xu, H.R. Ma, D.H. Sun, J. Gao, Catal. Lett. 45 (1997) 237–244.
[13] L. Li, Y. Yoshinaga, T. Okuhara, Phys. Chem. Chem. Phys. 1 (1999) 4913–4918.
[14] K. Tanabe, Mater. Chem. Phys. 13 (1985) 347–364.